

MARS PHASE REDDENING AND VNIR SPECTRAL DIVERSITY FROM ORBIT AS SEEN BY CaSSIS.

A. Valantinas¹, N. Thomas¹, A. Pommerol¹, L. Tornabene², G. Munaretto³ and the CaSSIS team. ¹Physikalisches Institut, Universität Bern, Sidlerstrasse 5, 3012 Bern, Switzerland (adomas.valantinas@unibe.ch), ²Inst. Space & Earth Exploration, Dept. Earth Sci., Western University, London, Canada, ³Astronomical Observatory of Padova (OAPD), INAF, Italy.

Introduction: Investigation in the visual to near infrared wavelengths (VNIR) of the surface spectral characteristics of Mars offers insights into its diverse geological history [1]. In particular, the analysis of the spectra taken under varying observation geometries can reveal further information about the surface composition and microstructure as was demonstrated by studies of the Moon [2], asteroids [3], and planetary regolith simulants in the laboratory [4-6]. Observations of Martian soil by the Viking 1 lander showed a substantial reddening and then bluing with increasing solar phase angle [7]. This trend has also recently been observed by the Mars Exploration Rovers (i.e., Spirit and Opportunity) [8]. However, orbital studies of this phenomenon were not possible in the past due to the fact that most Mars-orbiting spacecraft are in Sun-synchronous orbits. Here we analyze new multi-angular observations acquired by the Colour and Stereo Surface Imaging System (CaSSIS) [9] onboard the ExoMars Trace Gas Orbiter (TGO) to study the spectral properties of various materials found in Arabia Terra, Tharsis, Valles Marineris and Noachian highlands. Given TGO's non-Sun-synchronous orbit, CaSSIS can observe at a wide range of illumination geometries (0 to 90° phase). Additionally, we use CaSSIS band ratio spectra (e.g. NIR/BLU, PAN/BLU and PAN/NIR) to analyze different geologic units and to determine if these data can be used to identify minerals in new locations where CRISM observations are not available. The majority of the selected sites in this study were based on OMEGA-CRISM confirmed mineral detections [10,11].

Methods: Using Environment for Visualizing Images (ENVI) software we examined ~150 individual CaSSIS cubes, which featured either: 1) particulates (e.g. dust, sand and talus slope materials) or 2) rocky mineral (e.g. chlorides and phyllosilicates) regions of interest (ROIs). The distinction between these two categories was based on geologic context and THEMIS day/night IR maps [12]. The majority of ROIs were over 100 pixels in size (at 4.5 m/px resolution) and sampled the same materials but found in different locations on Mars. We also use the latest CaSSIS absolute and radiometric calibration, which offers photometric accuracy within ~2.8% [13,14]. For dust analysis we selected Arabia Terra and Tharsis because these regions are homogenous, very bright and predicted to be composed of particles a few micron in size [15].

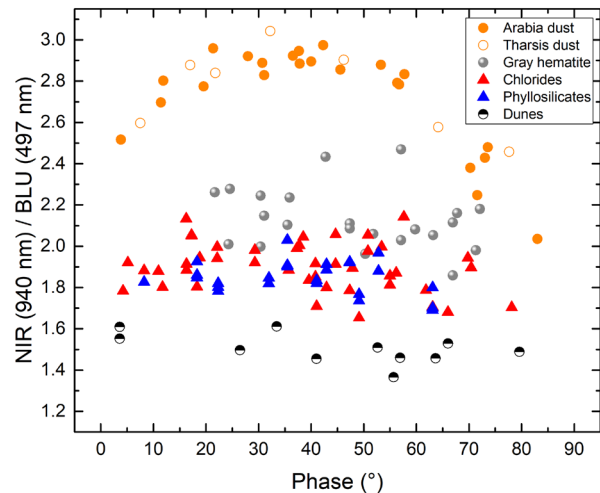


Figure 1. NIR/BLU spectral ratios plotted as a function of phase angle for particulate (circles) and rocky materials (triangles). Each data point is a different CaSSIS observation. The arch-shaped plot of dust from Arabia and Tharsis regions indicates dependence on phase angle, which is known as phase reddening/bluing effect.

Barchan sand dunes in the Martian highlands offer particle size ranges possibly from hundreds of microns up to a millimeter in size [16]. Lag deposits of gray crystalline hematite found on talus slopes of sulfate-rich walls of Valles Marineris are estimated to be >10µm or larger if they form polycrystalline aggregates [17]. Finally, phyllosilicate and chloride ROIs were compiled from old Noachian-aged terrains because they offer spectral characteristics and chemical alteration different from the aforementioned Martian loose soils [11].

Results: CaSSIS observations (see Fig. 1 uppermost plot) show that dusty regions of Arabia and Tharsis follow an arch-shaped (i.e., increase and decrease in NIR/BLU ratio values) phase curve indicative of the phase reddening/bluing effect. The arch peaks at roughly 40° phase and exhibits a sharp fall-off towards very large phase angles. The same trend cannot be observed for gray hematite and sandy dune materials. The latter show no dependence on phase angle, although hematite data points appear to be more scattered, which could indicate variable composition and/or particle size. Phyllosilicates and chlorides also do not show a dependence on phase angle, which is expected because of their (assumed) non-particulate nature.

CaSSIS band ratio plots (Fig. 2) indicate that each investigated material form a distinct group. For example, note the division between red ferric (dust, high PAN/BLU ratio) and blue ferrous (sand, low PAN/BLU ratio) materials. As in Fig. 1, the gray hematite data points exhibit the most scatter. Furthermore, the wide distribution of Tharsis and Arabia data points is due to the strong spectral ratio dependence on phase angle (i.e. phase reddening). Intriguingly, two observations in Fig. 2 indicate a very “blue” dust (low PAN/BLU ratio). Lastly, phyllosilicates and chlorides are centered around PAN/BLU values of 1.7, with the separation being more emphasized by the PAN/NIR ratio, which is expected from their known spectral characteristics [10].

Discussion: The observed arch (and its absence) in spectral ratios suggest that there are physical differences between the analyzed surface materials on particle size scales. From laboratory studies it is known that phase reddening of a given material depends on particle transparency, roughness and size [6]. Therefore the granular materials that make up barchan dunes and gray hematite deposits perhaps are opaque and consist of larger, and rougher particles than the surface fines found in homogenous regions of Arabia and Tharsis. Moreover it is plausible that surfaces of high topographic roughness do not exhibit phase reddening effects. Our observations also show that the phase curve peaks at around 40° for materials found in Arabia and Tharsis, which is lower than for crushed basalt samples ($\sim 80^\circ$) [5] and Martian soils found in Meridiani Planum, and Gusev crater ($45\text{--}75^\circ$) [8]. The latter may be attributed to differences in particle-scale roughness and surface scattering [8].

The two outlier observations of dust in Arabia (PAN/BLU value of 1.6 and 1.8) were taken in early morning and late evening respectively, and manual inspection reveals both scenes to be slightly bluer. These observations raise the possibility for presence of hypothesized ephemeral frost during Martian dusk and dawn [18]. Further monitoring of these locations and comparison to observations taken at later local solar times might provide additional clues about such diurnal processes.

Since our observations were based on ROIs sampled globally, it is likely that significant mineralogical differences exist (e.g. for non-homogenous regions such as Arabia or Tharsis) due to maturity and/or chemical weathering. The latter would explain the observed variation of hematite values in Fig. 1&2.

Future work: We plan to expand this study for other bright and dusty regions such as Elysium Planitia, which could help to distinguish between either pyroclastic or aeolian nature of the Cerberus Fossae mantling unit [19]. Also laboratory work at University

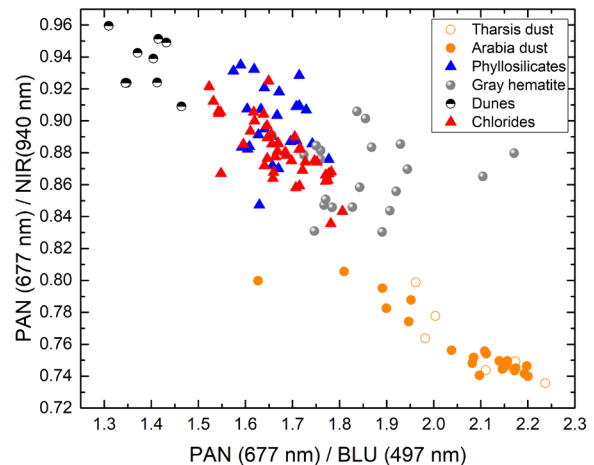


Figure 2. PAN/NIR vs PAN/BLU spectral ratios plotted for particulate (circles) and rocky materials (triangles). Note the division between ferric (nanophase iron dust) and ferrous (olivine-rich sand dune) materials.

of Bern is underway to investigate the effects of rock and dust mixtures on spectral ratios. Similar to the methods of [6] ray-tracing simulations may be applied to investigate the particle composition of Martian soils in locations with CaSSIS coverage.

References: [1] Ehlmann B.L. & Edwards C.S. (2014) *Annu. Rev. Earth Planet. Sci.* 42:291–315. [2] Gehrels T. et al. (1964) *Astron. J.*, 69, 826–852. [3] Taylor R.C. et al. (1971) *Astron. J.*, 76, 141–146. [4] Johnson J.R. et al. (2013) *Icarus*, 223, 383–406. [5] Pommerol A. et al. (2013) *JGR*, 118, 2045–2072. [6] Schröder S.E. et al. (2014) *Icarus*, 239, 201–216. [7] Guinness E.A. (1981) *JGR*, 86, 7983–7992. [8] Johnson J.R. et al. (2021) *Icarus*, 357, 114261. [9] Thomas N. et al. (2017) *Space Sci. Rev.* 212, 1897–1944. [10] Viviano-Beck C.E. et al. (2014) *JGR*, 119, 1403–1431. [11] Carter J.F. et al. (2013) *JGR*, 118, 831–858. [12] Hill J. et al. (2014) 8th International Conference on Mars, #1141. [13] Thomas N. et al. (2022) *PSS*, 211, 105394. [14] Pommerol A. et al. (in review) *PSS*. [15] Ruff S.W. & Christensen P.R. (2002) *JGR*, 107(E12), 5119. [16] Johnson J. R. et al. (2017) *JGR*, 122, 2655–2684. [17] Christensen P.R. et al. (2000) *JGR*, 105, 9623–9642. [18] Piqueux S. et al. (2016) *JGR*, 121, 1174–1189. [19] Horvath D.G. et al. (2021) *Icarus*, 365, 114499.

Acknowledgments: CaSSIS is a project of the University of Bern and funded through the Swiss Space Office via ESA's PRODEX programme. The instrument hardware development was also supported by the Italian Space Agency (ASI) (ASI-INAF agreement no.2020-17-HH.0), INAF/Astronomical Observatory of Padova, and the Space Research Center (CBK) in Warsaw. Support from SGF (Budapest), the University of Arizona (Lunar and Planetary Lab.) and NASA are also gratefully acknowledged. Operations support from the UK Space Agency under grant ST/R003025/1 is also acknowledged.